

Supplemental material for: Bilayers of Janus/Homogeneous Particle Mixtures Trapped at the Air/Water Interface

Anna Kozina,^{1,*} Salvador Ramos,² Pedro Díaz-Leyva,³ and Rolando Castillo²

¹*Instituto de Química, Universidad Nacional Autónoma de México, P. O. Box 70-213, 04510, Mexico City, Mexico*

²*Instituto de Física, Universidad Nacional Autónoma de México, P. O. Box 20-364, 01000, Mexico City, Mexico*

³*Departamento de Física, Universidad Autónoma Metropolitana Iztapalapa, San Rafael Atlixco 186, 09340 Mexico City, Mexico*

A. Additional Images

Fig. 1 shows more images of JP1/hydrophobic particle mixtures taken from different areas. “Flower-like” structures and “pillars” may be observed.

Fig. 2 shows the areas of the monolayer made by only JP2. Fluorescence images in Figs. 2 (b) and (e) strongly suggest that the orientation of Janus particles is not always the one of equilibrium (when the hydrophilic hemisphere is completely in water and the hydrophobic one is in the air). This is clear from the different brightness of fluorescence due to variation in the particle tilt. At least 50% of particles are tilted. The observation of non-equilibrium orientations suggests that these particles may deform the interface in the way described in Ref. [2], where this orientation is imposed. Therefore, although one would expect that Janus particles should rotate to the equilibrium orientation, we observe the opposite, they do not rotate, their rotational motion is arrested.

For comparison with Fig. 2 for fluorescent JP2, Fig. 3 shows homogeneously superficially modified fluorescent particles, equivalent to the marked hemisphere of JP2. The fluorescence images in Fig. 3 are completely different from those in Fig. 2. Homogeneous particles do not have variation in the fluorescence intensity, because they all are

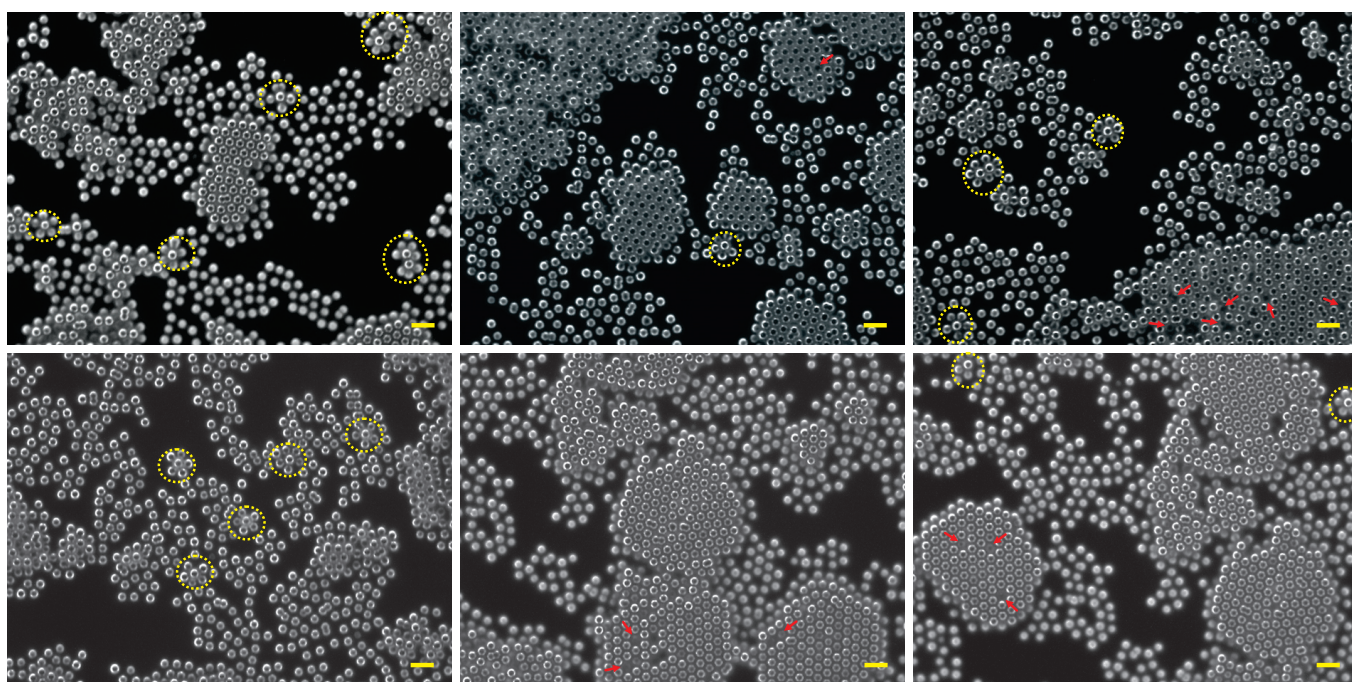


FIG. 1: Dark-field optical microscopy images of JP1/hydrophobic particle mixtures taken from different areas; “flowers” are marked by the circles, while pillars are marked by the red arrows; bars = 10 μm .

*To whom correspondence must be addressed: akozina@unam.mx

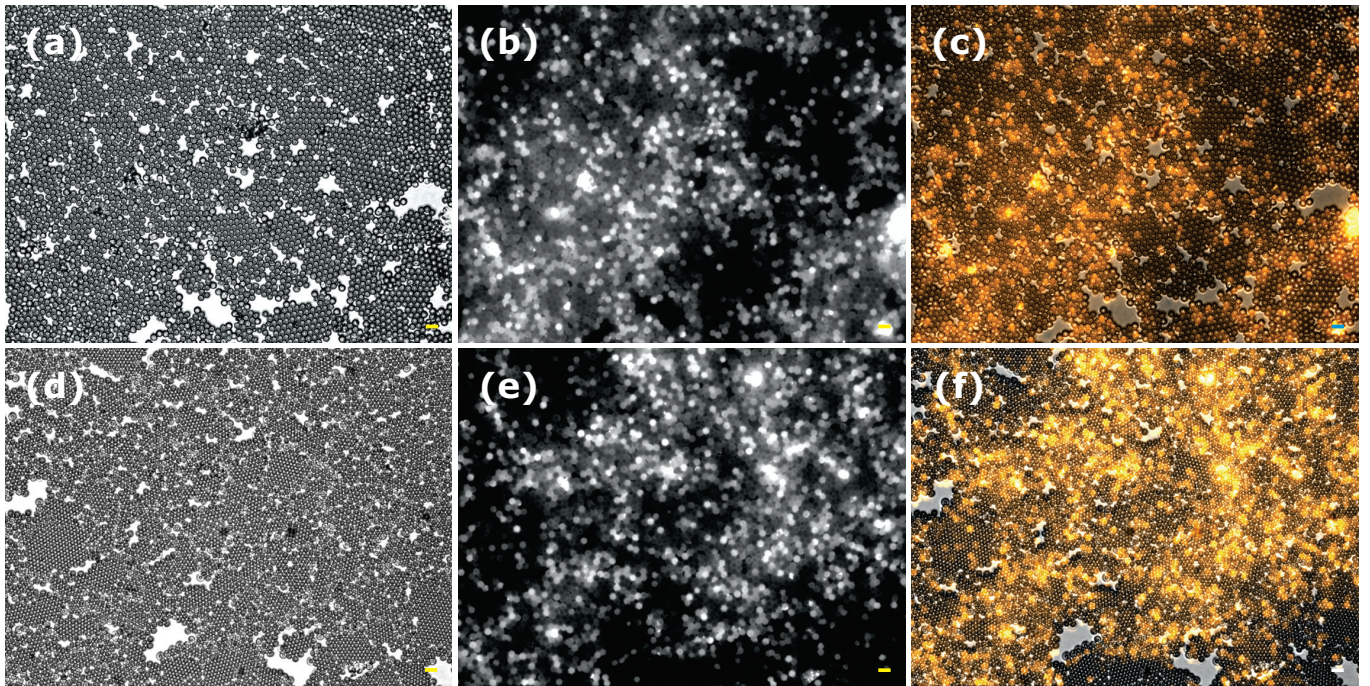


FIG. 2: Optical microscopy images of JP2 particles, (a) and (d) are bright-field images, (b) and (e) are fluorescence images, and (c) and (f) are overlaps of the bright-field and fluorescence adding an artificial colour to fluorescence; bars = $10 \mu\text{m}$.

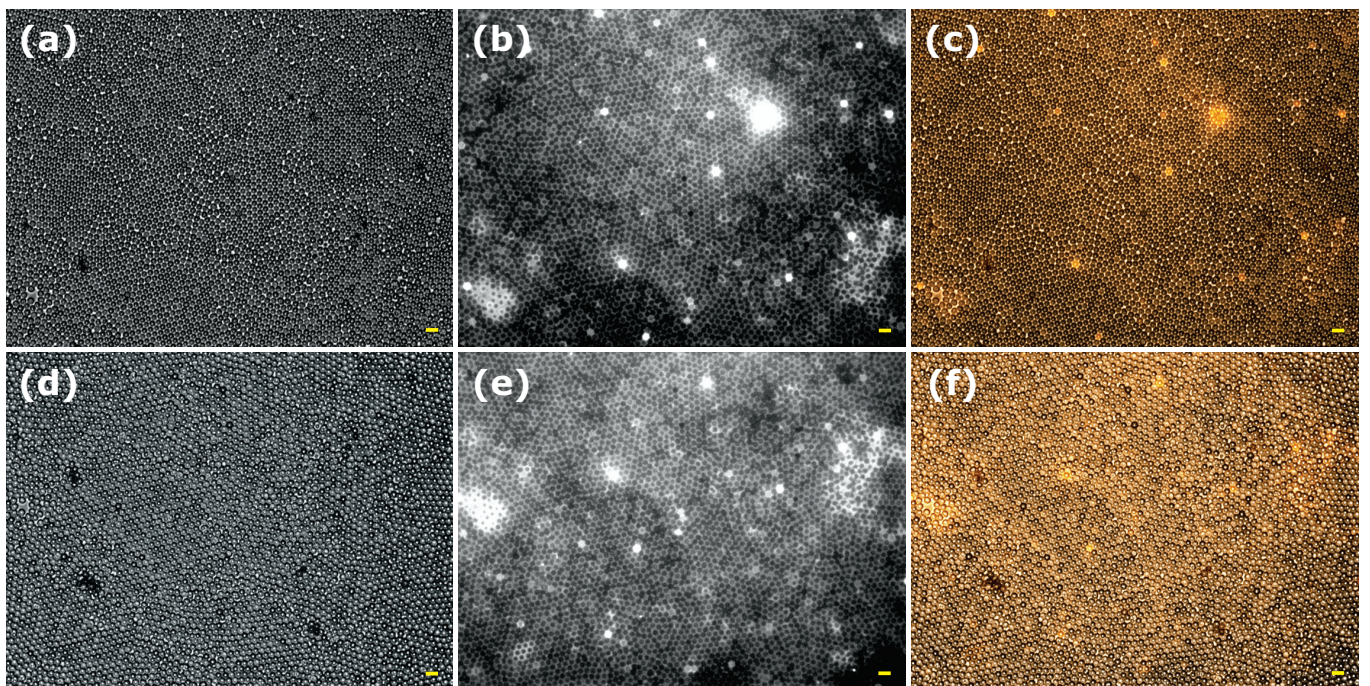


FIG. 3: Optical microscopy images of hydrophilic homogeneously marked particles, (a) and (d) are bright-field images, (b) and (e) are fluorescence images, and (c) and (f) are overlaps of the bright-field and fluorescence adding an artificial colour to fluorescence; bars = $10 \mu\text{m}$.

almost equally fluorescent and do not have any preferable orientation.

Fig. 4 shows other areas of the bilayer as seen in both bright field and fluorescence.

Fig. 5 shows another area of the bilayer as seen from above (dark field) and from below (bright field) by the two aligned optical microscopes.

Fig. 6 shows the images of the Janus/hydrophobic particle mixtures trapped at the a/o interface (here toluene is used as an oil instead of chloroform to avoid rapid evaporation, $\gamma^{tol} = 28.4$ mN/m at 20 °C; $\gamma^{chl} = 27.5$ mN/m at 20 °C). The suspension is spread from the toluene onto the clean toluene surface. As one can see from Figs. 6 (a) and (b), no bilayers are observed at the a/o interface. The particles have a vertical mismatch in the monolayer due to the difference in their three-phase contact angle. JPs are expected to be the bright ones. The hydrophobic particles look darker because more than a half of their volume is immersed into the oil phase. Figs. 6 (c) and (d) compare the same regions taken in the bright field and fluorescence. The darker regions in (c) correspond to the up-shifted particles and are the most fluorescent as shown in (d). Therefore, indeed, JPs are shifted up relatively to the hydrophobic ones when trapped at the a/o interface.

Fig. 7 shows the images of the Janus/hydrophobic particle mixtures trapped at the a/w interface using toluene as a spreading solvent. As one can observe in Fig. 7, there is no bilayer formed. A small z-shift may be due to the difference in the particle three-phase contact angles. Although there are some hexagonally packed regions, they do not have pronounced brightness contrast as seen in the bright field. Fluorescent images also do not show the JPs being only in the hexagonal clusters. Rather, they are distributed randomly among the hydrophobic non-fluorescent spheres. We suggest that this occurs for the following reasons. First, the diffusion does not compete with the solvent evaporation; therefore, the particles may reach the o/w interface more freely. Second, the sedimentation due to gravity matters. Third, the particles that are situated at the o/w interface do not freeze in the same way as at the a/w interface due to the lower toluene-water interfacial tension (weaker capillary interaction). Thus, they can rearrange before the toluene evaporation is complete. Generally, it seems like on spreading from toluene the system may relax easier and get closer to the equilibrium spreading conditions. Also, the particle organization resembles the one in Fig. 6. It seems like the structure is slowly transferred from the a/o to the a/w interface as the solvent evaporates. Therefore, as mentioned in the manuscript, the kinetics of the spreading solvent evaporation are decisive in the bilayer formation.

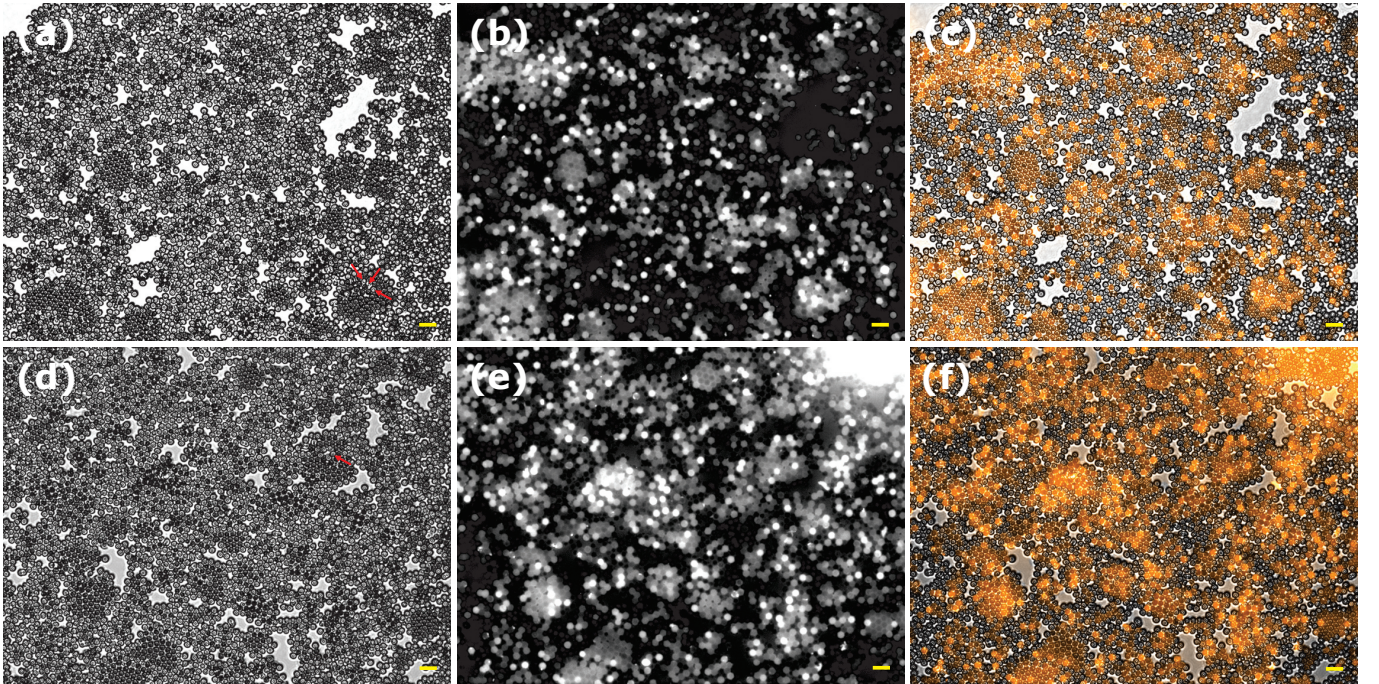


FIG. 4: Optical microscopy images of JP2/hydrophobic particle mixtures. Each row corresponds to a certain a/w interface region. (a) and (d) are bright-field images, (b) and (e) are fluorescence images, and (c) and (f) are overlaps of the bright field and fluorescence adding an artificial colour to fluorescence. Red arrows denote “pillars” made of hydrophobic particles. Bars = 10 μ m.

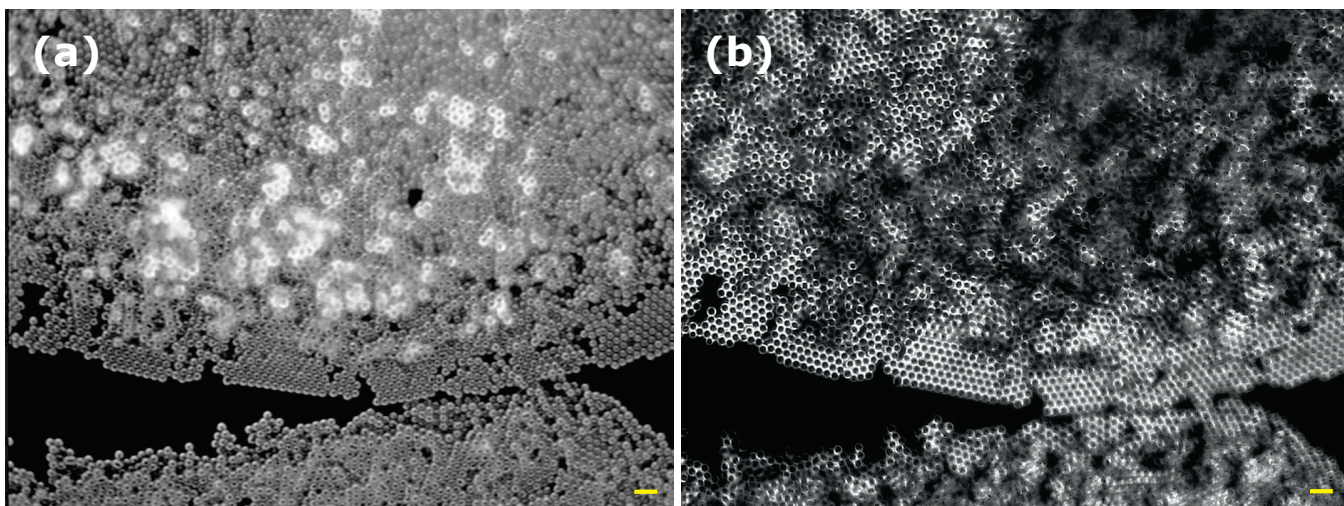


FIG. 5: Optical microscopy images of JP1/hydrophobic particle mixtures: (a) the dark-field image as seen from above; (b) the corresponding bright-field image as seen from below. Bars = 10 μm .

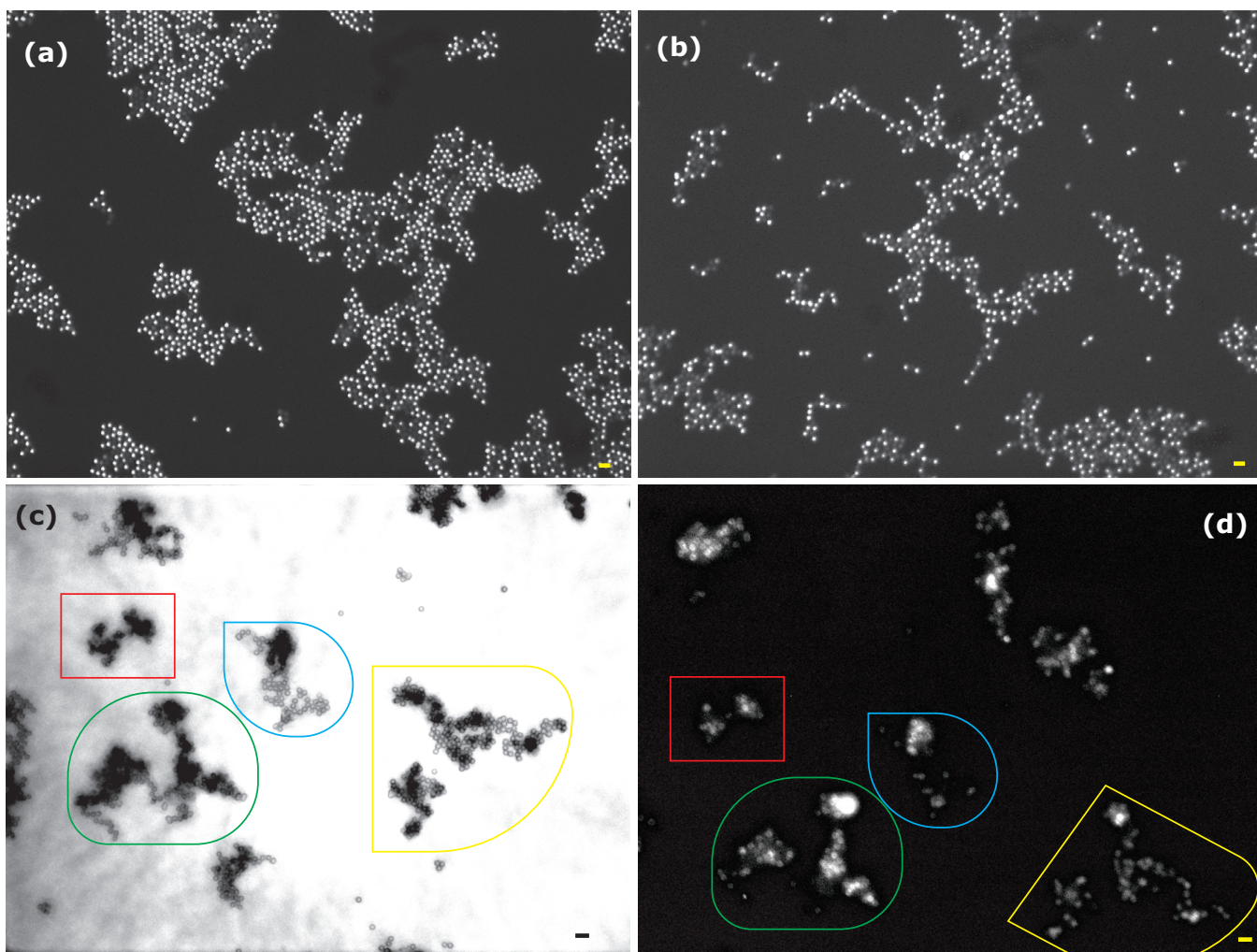


FIG. 6: Optical microscopy images of Janus/hydrophobic particle mixtures: (a) and (b) are the dark-field images of the two different regions, JP1 are used, (c) is the bright-field image and (d) is the corresponding fluorescence image, JP2 are used. Colour shapes are guides for the eye. Bars = 10 μm .

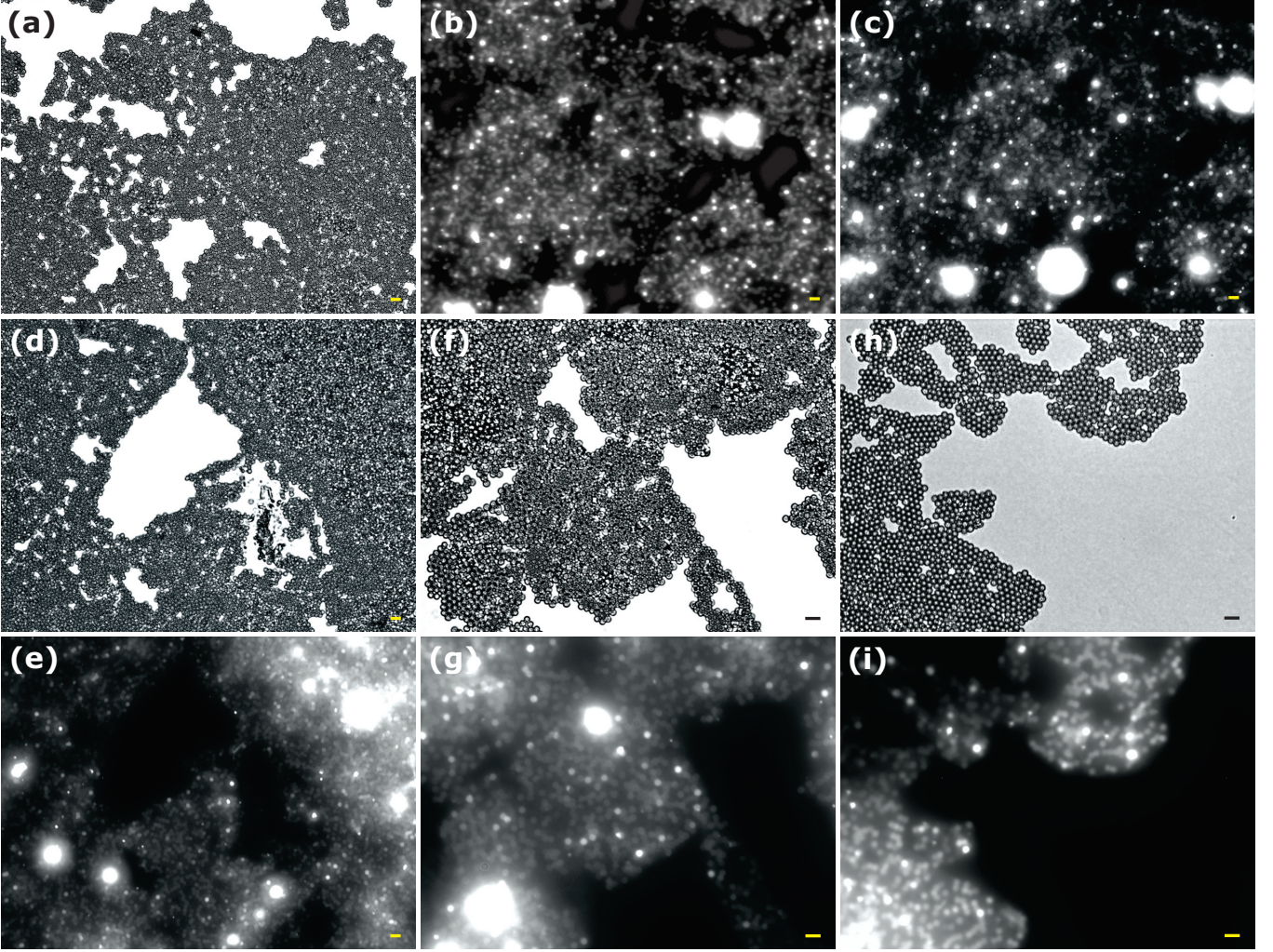


FIG. 7: Optical microscopy images of JP1/hydrophobic particle mixtures spread from toluene: (a), (b) and (c); (d) and (e); (f) and (g); (h) and (i) correspond to the same area taken in the bright field and fluorescence (some of them are a bit shifted due to convection). Bars = 10 μm .

B. Calculation of the Interface Desorption Energy

The energy of desorption of a Janus particle of radius R from an interface into the oil $E(\alpha)_{oil}$ or water $E(\alpha)_{water}$ phase is given by [1]:

$$E(\alpha)_{oil} = 2\pi R^2 \gamma_{ow} \left[\frac{\sin^2 \alpha}{2} + \cos \theta_P^{o/w} (\cos \alpha - 1) \right], \quad (1)$$

$$E(\alpha)_{water} = 2\pi R^2 \gamma_{ow} \left[\frac{\sin^2 \alpha}{2} + \cos \theta_A^{o/w} (\cos \alpha + 1) \right], \quad (2)$$

where γ_{ow} is the oil/water interfacial tension, for toluene/water interface $\gamma_{ow} = 35$ mN/m; α is the angle that defines the polar and apolar parts of the Janus sphere; $\theta_P^{o/w} = 130^\circ$ and $\theta_A^{o/w} = 70^\circ$ are the polar and apolar particle contact angles at the o/w interface, respectively (see Fig. 5 (a) of the main text). For the air/oil interface the Eqs. 1 and 2 hold by substitution of γ_{ow} by toluene surface tension $\gamma^{tol} = 28.4$ mN/m and the corresponding particle contact angles at the air/oil interface $\theta_P^{a/o} = 60^\circ$ and $\theta_A^{a/o} = 90^\circ$. Angle α is varied in the range $\theta_A < \alpha < \theta_P$ and therefore α is also the contact angle of the Janus particle.

For the homogeneous hydrophobic particles Eqs. 1 and 2 simplify to

$$E(\alpha)_{oil} = 2\pi R^2 \gamma_{ow} (1 - \cos \theta_A^{o/w})^2, \quad (3)$$

$$E(\alpha)_{water} = 2\pi R^2 \gamma_{ow} (1 + \cos \theta_A^{o/w})^2, \quad (4)$$

Again, for the air/oil interface the corresponding contact angle $\theta_A^{a/o}$ is used.

C. Videos

Movie-1. Video of a z -stack of the area different from the reported in the main text. Each new frame corresponds to the vertical shift of $0.5 \mu\text{m}$ from up to down of the bilayer.

-
- [1] S. Jiang, S. Granick, J. Chem. Phys. **127**, 161102 (2007).
 [2] H. Rezvantalab, S. Shojaei-Zadeh, Soft Matter **9**, 3640-3650 (2013).